

High-Order Sliding Mode Control for the Test Mass stabilization of the LISA Mission: preliminary results

*Original*

High-Order Sliding Mode Control for the Test Mass stabilization of the LISA Mission: preliminary results / Bloise, Nicoletta; Capello, Elisa; Punta, Elisabetta; Grzymisch, Jonathan. - (2021). (Intervento presentato al convegno International ESA Conference on Guidance, Navigation & Control Systems).

*Availability:*

This version is available at: 11583/2970208 since: 2022-07-21T08:46:45Z

*Publisher:*

ESA Publications Division

*Published*

DOI:

*Terms of use:*

This article is made available under terms and conditions as specified in the corresponding bibliographic description in the repository

*Publisher copyright*

(Article begins on next page)

# HIGH-ORDER SLIDING MODE CONTROLLER FOR THE TEST MASS STABILIZATION OF THE LISA MISSION: PRELIMINARY RESULTS \*

Nicoletta Bloise<sup>(1)</sup>, Elisa Capello<sup>(1),(2)</sup>, Elisabetta Punta<sup>(2)</sup>, Jonathan Grzymisch<sup>(3)</sup>

<sup>(1)</sup> *Department of Mechanical and Aerospace Engineering, Politecnico di Torino, Corso Duca degli Abruzzi 24, 10129 Torino, Italy, nicoletta.bloise@polito.it, elisa.capello@polito.it*

<sup>(2)</sup> *CNR-IEIIT, Politecnico di Torino, Corso Duca degli Abruzzi 24, 10129 Torino, Italy, elisabetta.punta@ieiit.cnr.it*

<sup>3</sup> *ESA, European Space Research and Technology Centre, Keplerlaan 1, Noordwijk, The Netherlands, Jonathan.Grzymisch@esa.int*

## ABSTRACT

The main objective of this paper is the design of a controller for the test mass release of the Laser Interferometer Space Antenna (LISA) mission. Since the test masses are used as sensors in the science phase for environmental measurements, the control system can be able to robustly deal with large initial deviations of the release mechanism. Moreover, the control system should be able to maintain and stabilize the test masses with a precision. For this reason, two Sliding Mode Control (SMC) are included in this study. A second-order SMC is mainly proposed for this critical phase, which is able to handle uncertainties and noise introduced by the sensors system. This controller is compared with a first-order SMC, which was used in LISA Pathfinder mission, in terms of accuracy and steady-state error. A nonlinear orbital simulator is considered in the simulations, with limitations both of the actuation system (with saturation and delay) and of the update frequencies. Model uncertainties, different initial conditions and external disturbances are also included in the performed simulations.

## 1 INTRODUCTION

LISA mission is selected to be ESA's third large-class mission with a launch planned in 2034 and a duration time of 5 years. The main goal of this mission is to realize a space gravitational observatories will be complementary to the existing terrestrial laboratories to detect gravitational low frequency signals, not measurable from Earth. In 2015, LISA Pathfinder's pioneering mission is launched by ESA to test key technologies required to satisfy LISA performance requirements and the results are reported in [1, 2]. LISA Pathfinder was dedicated to carry out experimental demonstration in view of the subsequent LISA mission, expected in 2034. The LISA mission consists of different phases and the spacecraft are equipped with a Drag Free and Attitude Control System (DFACS), which compensates for the non-gravitational disturbances and guarantee free fall conditions. In [3], the authors present a preliminary study on DFACS for the science phases of the LISA mission and they detailed the simulator model used for the definition of the control system. In general, as deeply described in [4], several strict requirements are given from LISA Pathfinder mission, in particular for the initial conditions.

---

\*This work was supported by the European Space Agency.

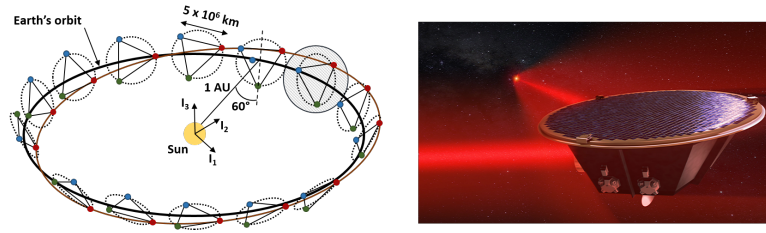


Figure 1: LISA Mission Constellation and its spacecraft

The main focus of this paper is phase of test mass release, in which the control system should steer and keep the test mass at the center of the case, for measuring the gravitational waves. Since in this phase the robustness of the control system is a key feature, as for Lisa Pathfinder, Sliding Mode Control (SMC) techniques are proposed to guarantee stringent requirements, even with parameters other than nominal ones. SMC control systems are widely designed in space applications, as in [5, 6, 7, 8]. In this paper, two SMC control strategies are compared: (1) a second order SMC algorithm, in detail Super-Twisting (STW), and (2) a first order SMC controller. The STW SMC, as in [9], is able to counteract disturbances and uncertainties and is less affected by chattering phenomenons. Extensive simulations are performed including different initial conditions and disturbances, with a limited control authority in a noisy and disturbed environment, to highlight the main difference and properties of the two control strategies.

The paper is organized as follows. In Section 2 the mission and the uncertainties are described. Section 3 dealt with sliding mode theory and the proposed first and second order SMC control systems. Then in Section 4 some simulation results are introduced. Finally, in Section 5 the conclusion are summarized.

## 2 LISA MISSION DESCRIPTION AND SYSTEMS

In particular, LISA observatory consists of a constellation of three spacecraft organized in an equilateral triangle with sides 2.5 million km long and is on near-circular Earth heliocentric, as shown in Figure 1. Each spacecraft contains two optical assemblies and two test masses, included in the laser interferometer (in a Michelson configuration). Test masses are gold-platinum cubes of 46 mm side with a weight of 1.96 kg. An important requirements of the mission is to protect the two test masses of each spacecraft against all external disturbances, to have free fall on their own geodesic. The relative distance of test mass, continually measured, changes when a gravitation wave passes through. Once the three spacecraft have been inserted into their correct orbits forming an observatory, science operations can start. This include the release of the Test Masses and engaging the DFACS. Following constellation acquisition and calibration, all TMs will be in free fall along the lines of sight between spacecraft and LISA enters in science mode. Finally, gravitational waves may be detected by measuring the change in relative distances between test-masses on different spacecraft, at pico-meter level. Thanks to LISA Pathfinder's pioneering mission, we are taken the initial state conditions of our problem from the estimated initial condition, as summarised in [4]. The controller of the test masses must be design to deal with large initial offsets and velocities for the position and attitude states.

A great challenge of this control system is given by the limited actuation authority of the electrostatic suspensions, which allow the application of electrostatic forces and torques to the test masses, which is the Gravitational Reference Sensor (GRS) and actuators. This system consists into an electrostatic actuation and is able to measure all the six degrees of freedom (DoFs) of the TMs. Two operational

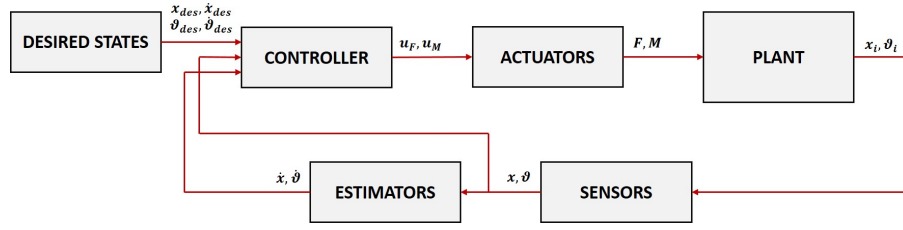


Figure 2: Simulator architecture

modes are provided by this actuation system: (1) one is related to the Wide Range (WR) mode of electrostatic suspensions, and (2) High Resolution (HR) mode is used to improve control accuracy. The first mode is active when the TM is released, since it allows higher forces but introduces more noises. In the second operational mode high accuracy and steady-state errors are required, to obtain good performance also in the science mode.

The analysis and related results are performed in a simulation environment, in which a nonlinear dynamics is implemented for the TMs and for the spacecraft. Moreover, the simulator takes into account several disturbances such as self gravity (SG), masses stiffness and noises from the GRS actuation systems. The main disturbance is applied as function of the maximum actuation authority, as detailed in [10].

The orbital simulator is illustrated in Figure 2 and it includes the following subsystems: (i) plant dynamics of spacecraft and test mass, (2) sensor model to obtain the measured values of the positions and attitude angles, and (3) a state estimator for the observation of the velocities. The error dynamics, which is the difference between the states and the desired values, is the input of the control system. The controller is designed considering this error dynamics and to stabilize the TMs. The strict limits of the actuation system are included to evaluate the force and torque to be applied.

Moreover, parametric uncertainties are also included in the model, in terms of mass and inertia properties.

### 3 SLIDING MODE CONTROL

The sliding mode control is a nonlinear control approach [9, 11], able to ensure high accuracy and excellent robustness against external disturbances and parameter variations. It is designed to drive the system states onto a particular surface, named “sliding” surface. The sliding surface is calculated starting from the error between the sensor signals and the reference values.

Each TM has six DoF to be controlled (three for the position and three for the attitude), for each of which a sliding output is defined

$$\sigma_i = (\dot{\mathbf{x}}_i - \dot{\mathbf{x}}_{di}) + c_i(\mathbf{x}_i - \mathbf{x}_{di}), \quad i = 1, \dots, 6 \quad (1)$$

where  $c_i$ ,  $i = 1, \dots, 6$ , are positive constants. It is defined the vector  $\mathbf{x} = [\mathbf{x}_1, \mathbf{x}_2, \mathbf{x}_3, \mathbf{x}_4, \mathbf{x}_5, \mathbf{x}_6]^T = [x, y, z, \theta_x, \theta_y, \theta_z]^T \in R^6$ , and the vectors  $\mathbf{x}_d, \dot{\mathbf{x}}_d \in R^6$  contain respectively the desired position and attitude and translational and rotational velocities.

In the translational and rotational dynamics of each TM the control matrices are diagonal ones, therefore each of the six DoFs has a dedicated control input. For each TM it is defined a control vector  $\mathbf{u} = [\mathbf{u}_1, \mathbf{u}_2, \mathbf{u}_3, \mathbf{u}_4, \mathbf{u}_5, \mathbf{u}_6]^T \in R^6$ . The vectors of the forces  $F_E \in R^3$  and torques  $M_E \in R^3$  acting on the TM are the control inputs, i.e.  $\mathbf{u} = [F_E^T, M_E^T]^T$ .

The sliding variables  $\sigma_i$  in (1) have relative degree 1 with respect to  $\mathbf{u}_i$ ; the dynamics of each sliding

output  $\sigma_i$  can be expressed as

$$\dot{\sigma}_i = h_i(t, \mathbf{x}) + \mathbf{u}_i, \quad (2)$$

where the uncertain term  $h_i(t, \mathbf{x})$  is assumed bounded as well as its first order time derivative, i.e.,  $|h_i| < M_i$  and  $|\dot{h}_i| < L_i$  at least locally. The constant bounds  $M_i$  and  $L_i$  are assumed known.

### 3.1 Second Order Sliding Mode Control

We propose a second order SMC algorithm named Super-Twisting (STW) for both the position and attitude control system. STW designs a continuous control law, which is able to steer to zero in a finite time not only the sliding output, but also its first time derivative. A further advantage regards the chattering phenomenon, which is attenuated improving the control accuracy.

Each component of the control vector  $\mathbf{u}$  has been designed according to the second order STW SMC algorithm

$$\begin{aligned} \mathbf{u}_i &= -\lambda_i |\sigma_i|^{\frac{1}{2}} \text{sgn}(\sigma_i) + \mathbf{v}_i \\ \dot{\mathbf{v}}_i &= \begin{cases} -\mathbf{u}_i, & \text{if } |\mathbf{u}_i| > U_{Mi}, \\ -\alpha_i \text{sgn}(\sigma_i), & \text{if } |\mathbf{u}_i| < U_{Mi}, \end{cases} \quad i = 1, \dots, 6. \end{aligned} \quad (3)$$

where the sliding variable  $\sigma_i$  is defined in (1) and the control parameters are chosen such that  $\lambda_i > 1.5L_i^{\frac{1}{2}}$ ,  $\alpha_i > 1.1L_i$ , and  $q_i U_{Mi} > M_i$ ,  $0 < q_i < 1$ , with  $M_i > 0$  and  $L_i > 0$  known constant bounds of the uncertainties. The STW SMC strategy does not require the availability of any time derivative of the sliding variable. However, the design of the sliding surface relies on the knowledge of signals such as linear and angular velocities.

### 3.2 First Order Sliding Mode Control

Each component of the control vector  $\mathbf{u}$  has been designed according to the first order SMC law

$$\mathbf{u}_i = -K_i \text{sgn}(\sigma_i), \quad i = 1, \dots, 6, \quad (4)$$

where  $\sigma_i$  is the sliding variable in (1) and the control parameter  $K_i$  must be chosen such that  $K_i > M_i$ , with  $M_i > 0$  known constant bound of the uncertainty.

A first order SMC is proposed here indeed because a strategy of this kind was applied in Lisa Pathfinder. Therefore it is interesting to present the results of the second order STW-SMC algorithm compared to those of the first order SMC.

## 4 PRELIMINARY SIMULATION RESULTS

In this section, preliminary simulation results are exposed and a comparison between a first and second order SMC is proposed for the TM release. As previously mentioned, the objective of this study is to maintain test masses in the middle of the case with zero speed, this means that the desired states in term of position and velocity are equal zero. Exploiting the measured signals (affected by noise) of positions and attitude, the estimated velocities have been provided by using an approximation of the derivatives of each signal, smoothed by a low pass filter with desired bandwidth. Moreover, in this work, the action of the controller is limited due to the small force, that can be exerted by the electrostatic actuators and due to the constraint on the switching frequency, imposed by the actuation system, of 10 Hz. These two limitations reduce the accuracy of the controller itself, in terms of position and

Table 1: LISA Pathfinder initial conditions (ICs)

The initial state conditions in LISA Pathfinder				
Axis	Position/Attitude	Requirements	Velocity/Rate	Requirements
$x_2$	193.5 $\mu\text{m}$	$\pm 200 \mu\text{m}$	7.5 m/s	$\pm 5 \mu\text{m/s}$
$y_2$	-453.6 $\mu\text{m}$	$\pm 200 \mu\text{m}$	-22.3 m/s	$\pm 5 \mu\text{m/s}$
$z_2$	-250.3 $\mu\text{m}$	$\pm 200 \mu\text{m}$	-16.4 m/s	$\pm 5 \mu\text{m/s}$
$\phi_2$	15.4 mrad	$\pm 2 \text{ mrad}$	685 $\mu\text{rad/s}$	$\pm 100 \mu\text{rad/s}$
$\theta_2$	-1.1 mrad	$\pm 2 \text{ mrad}$	26.3 $\mu\text{rad/s}$	$\pm 100 \mu\text{rad/s}$
$\psi_2$	-4.3 mrad	$\pm 2 \text{ mrad}$	-250.7 $\mu\text{rad/s}$	$\pm 100 \mu\text{rad/s}$

velocity error [9, 12, 13]. We test the controller and the actuation system for the first 1000s in the WR mode, in which the GRS actuation force authority is about  $10^{-6}$  N and the GRS actuation torque authority is  $10^{-8}$  Nm. Then, automatically, to improve the steady-state error, GRS actuation switch in HR mode where force authority decreases to  $10^{-9}$  N and torque authority to  $10^{-11}$  Nm. Due to the low control authority, considering also the disturbances and the sensors noises, force and torque often saturate. To avoid maintenance and damage of the system, the saturation value are considered as 98% of the ideal maximum value. From [4], the initial conditions are defined as in Table 1. In particular, some values, highlighted in red, are considered critical, analyzing the LISA Pathfinder mission. Note that, since both TMs have the same characteristics, simulation results are shown only for TM1.

Starting from the ICs of Table 1, the performance of both STW-SMC control system and of a first order SMC are tested, including the two operative mode. As previously said, the steady state error in the HR Mode should be small due to the strict requirements for drag free science mode. As in Table 2, the obtained steady-state error is about  $10^{-6}$  m for the the positions and about  $10^{-7}$  m/s for the linear velocities, when the WR operative mode is considered. This behavior can be observed also in Figs. 3 and 4. Even if the initial conditions are strongly different from the desired values, the STW SMC is able to track the values with high precision, in both operative mode. For the HR mode, with the STW-SMC the steady-state error is reduced of two order of magnitude, with respect to the WR mode, even if the control authority is strongly reduced. Similar results are obtained with a first-order SMC. However, chattering can be observed in Figs. 5 and 6, and a higher settling time is observed.

Table 2: WR steady-state error for TM1 with a STW-SMC

WR	x-sup	x-inf	y-sup	y-inf	z-sup	z-inf
Position	1.487e-6	-1.487e-6	1.358e-6	-1.358e-6	1.701e-6	-1.701e-6
Linear Vel.	4.965e-7	-4.965e-7	4.378e-7	-4.378e-7	4.378e-7	-4.378e-7
Euler angle	1.754e-5	-1.754e-5	1.694e-5	-1.694e-5	1.697e-5	-1.697e-5
Angular Vel.	2.012e-5	-2.012e-5	1.058e-5	-1.058e-5	1.359e-5	-1.359e-5

Table 3: HR steady-state error for TM1 with a STW-SMC

HR	x-sup	x-inf	y-sup	y-inf	z-sup	z-inf
Position	1.188e-7	-1.188e-7	3.068e-7	-3.068e-7	2.673e-7	-2.673e-7
Linear Vel.	7.378e-9	-7.378e-9	5.915e-9	-5.915e-9	5.915e-9	-5.915e-9
Euler angle	3.249e-7	-3.249e-7	8.444e-7	-8.444e-7	2.608e-6	-2.608e-6
Angular Vel.	8.240e-8	-8.240e-8	7.700e-8	-7.700e-8	1.772e-7	-1.772e-7

## 5 CONCLUSIONS

In this paper, a SMC controller is proposed based on the Super-Twisting second-order SMC algorithm for the nonlinear control problem of the test mass release in the first phase of LISA mission. The

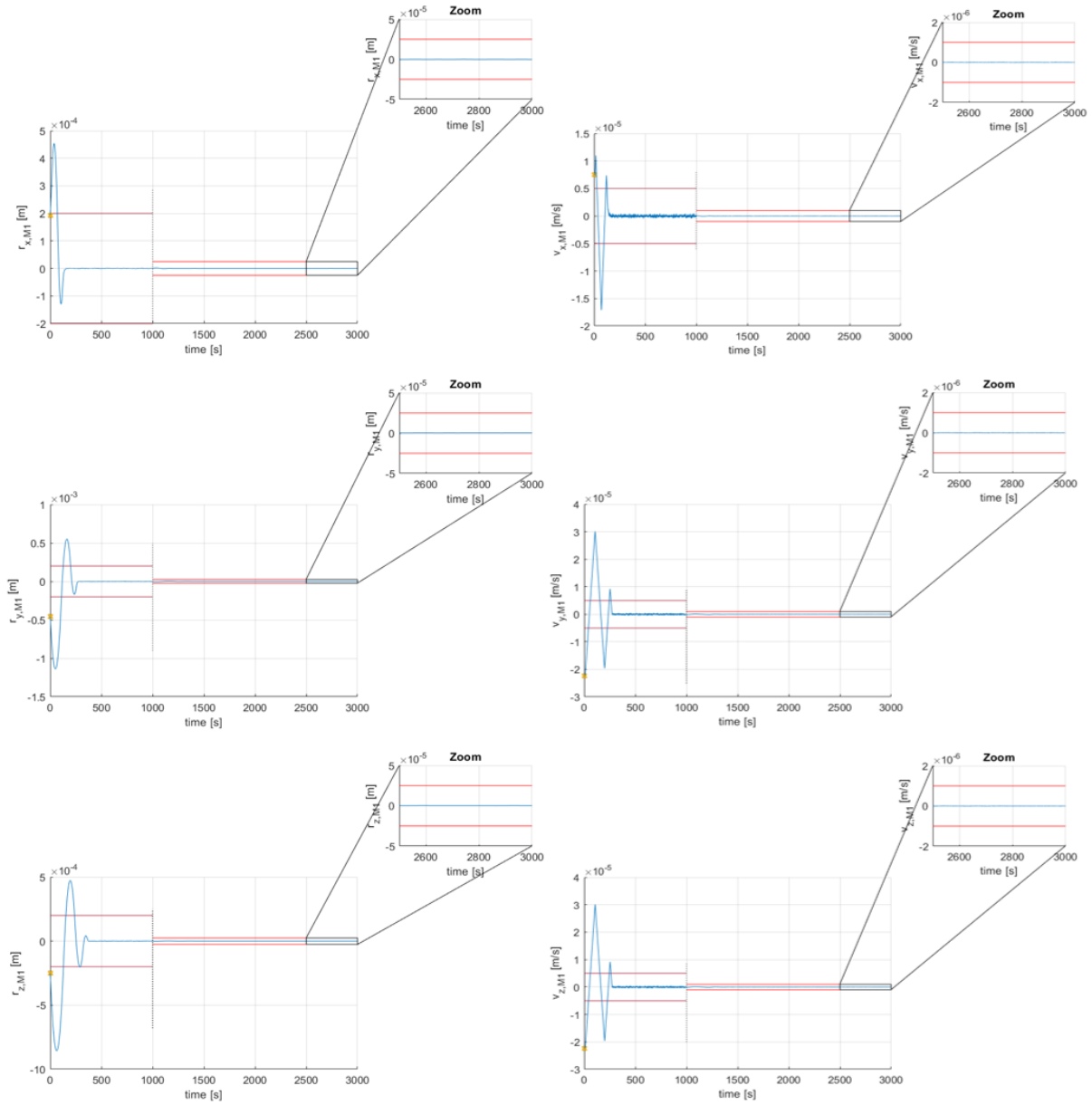


Figure 3: Position and linear velocities with a STW-SMC

Table 4: WR steady-state error for TM1 with a 1st order SMC

WR	x-sup	x-inf	y-sup	y-inf	z-sup	z-inf
Position	1.487e-6	-1.487e-6	1.358e-6	-1.358e-6	1.701e-6	-1.701e-6
Linear Vel.	4.965e-7	-4.965e-7	4.378e-7	-4.378e-7	4.378e-7	-4.378e-7
Euler angle	1.754e-5	-1.754e-5	1.694e-5	-1.694e-5	1.697e-5	-1.697e-5
Angular Vel.	2.012e-5	-2.012e-5	1.058e-5	-1.058e-5	1.359e-5	-1.359e-5

Table 5: HR steady-state error for TM1 with a 1st order SMC

HR	x-sup	x-inf	y-sup	y-inf	z-sup	z-inf
Position	1.188e-7	-1.188e-7	3.068e-7	-3.068e-7	2.673e-7	-2.673e-7
Linear Vel.	7.378e-9	-7.378e-9	5.915e-9	-5.915e-9	5.915e-9	-5.915e-9
Euler angle	3.249e-7	-3.249e-7	8.444e-7	-8.444e-7	2.608e-6	-2.608e-6
Angular Vel.	8.240e-8	-8.240e-8	7.700e-8	-7.700e-8	1.772e-7	-1.772e-7

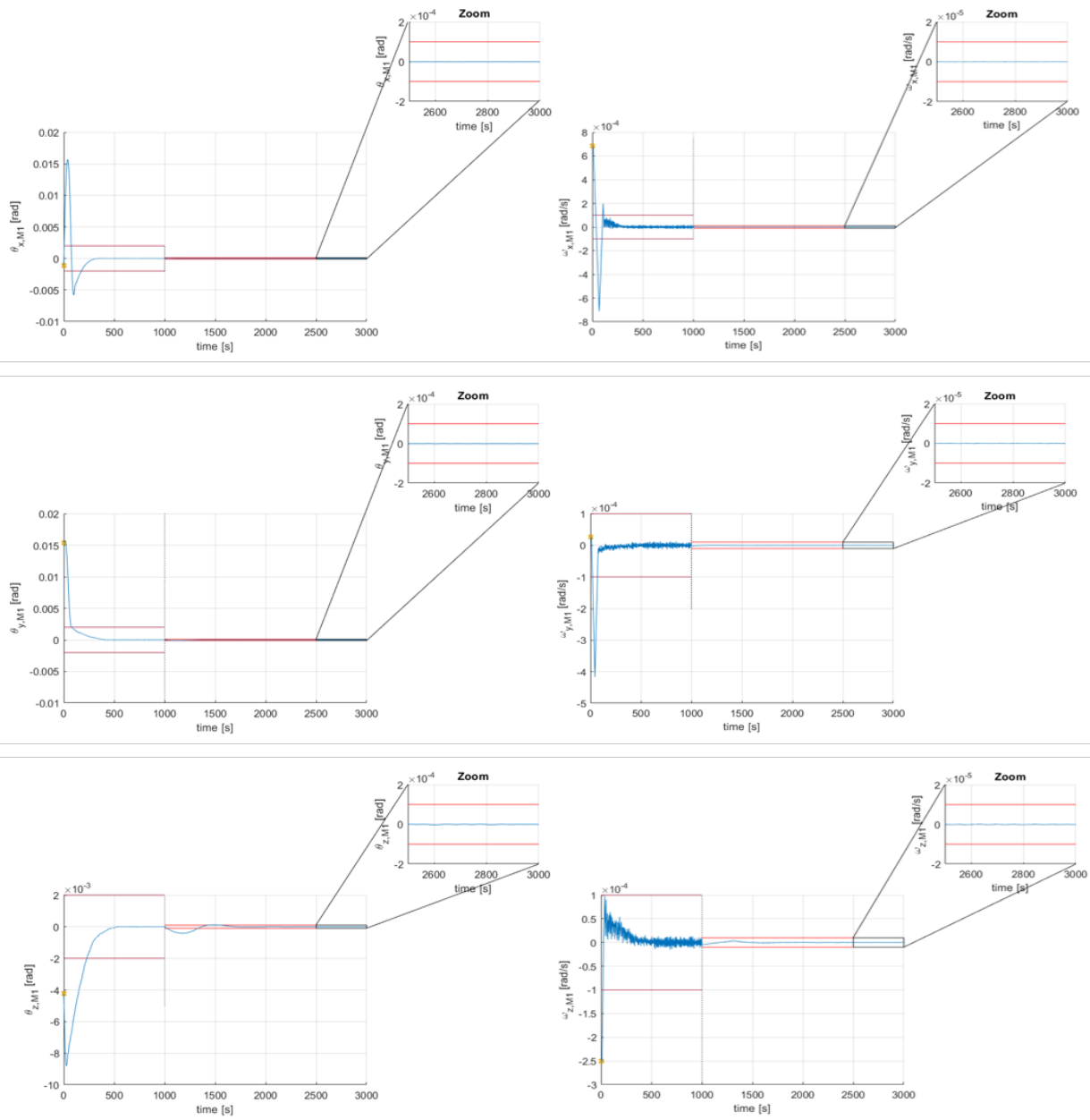


Figure 4: Euler angles and angular velocities with a STW-SMC



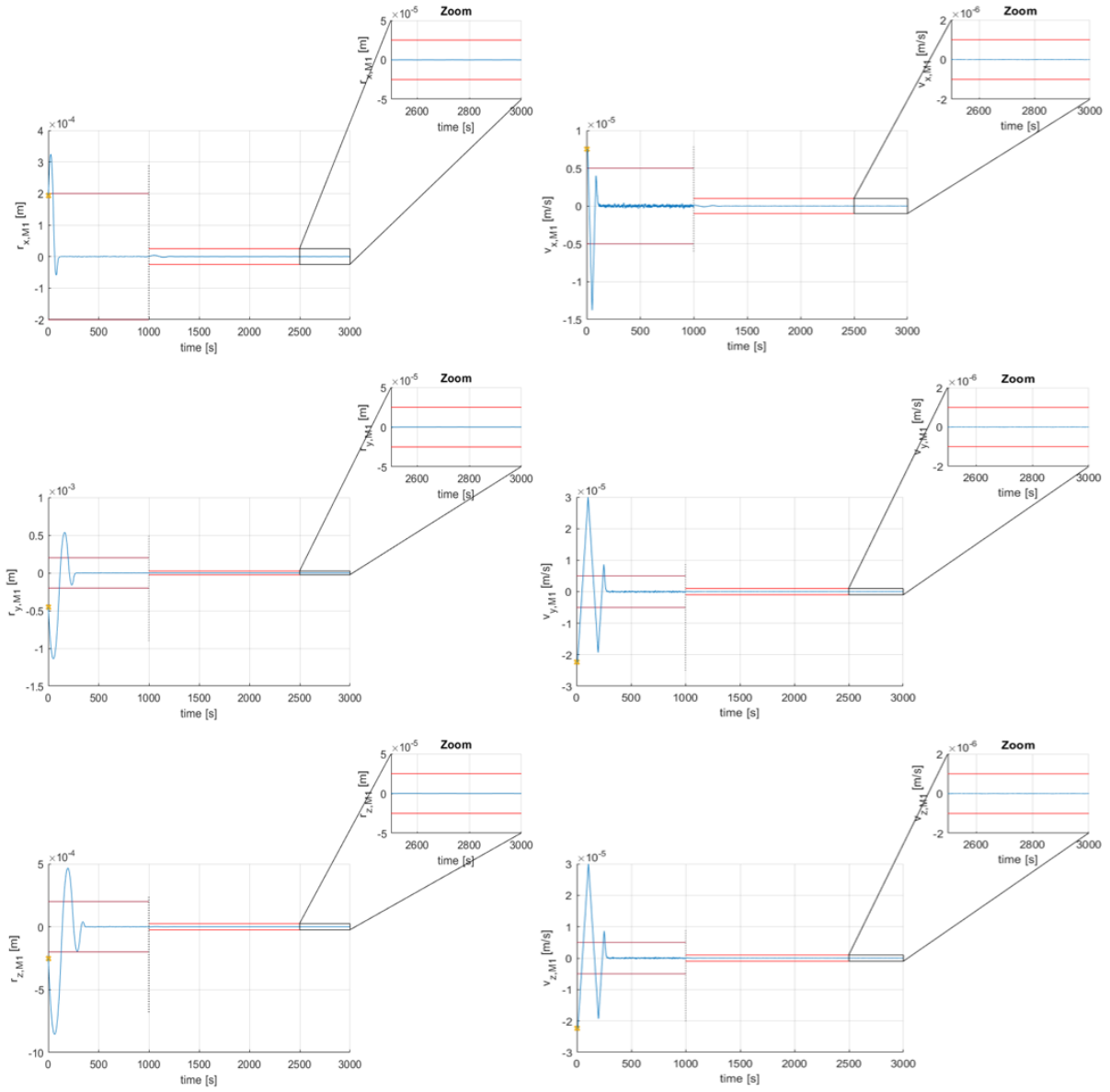


Figure 5: Variation of positions and linear velocities with a 1st order SMC

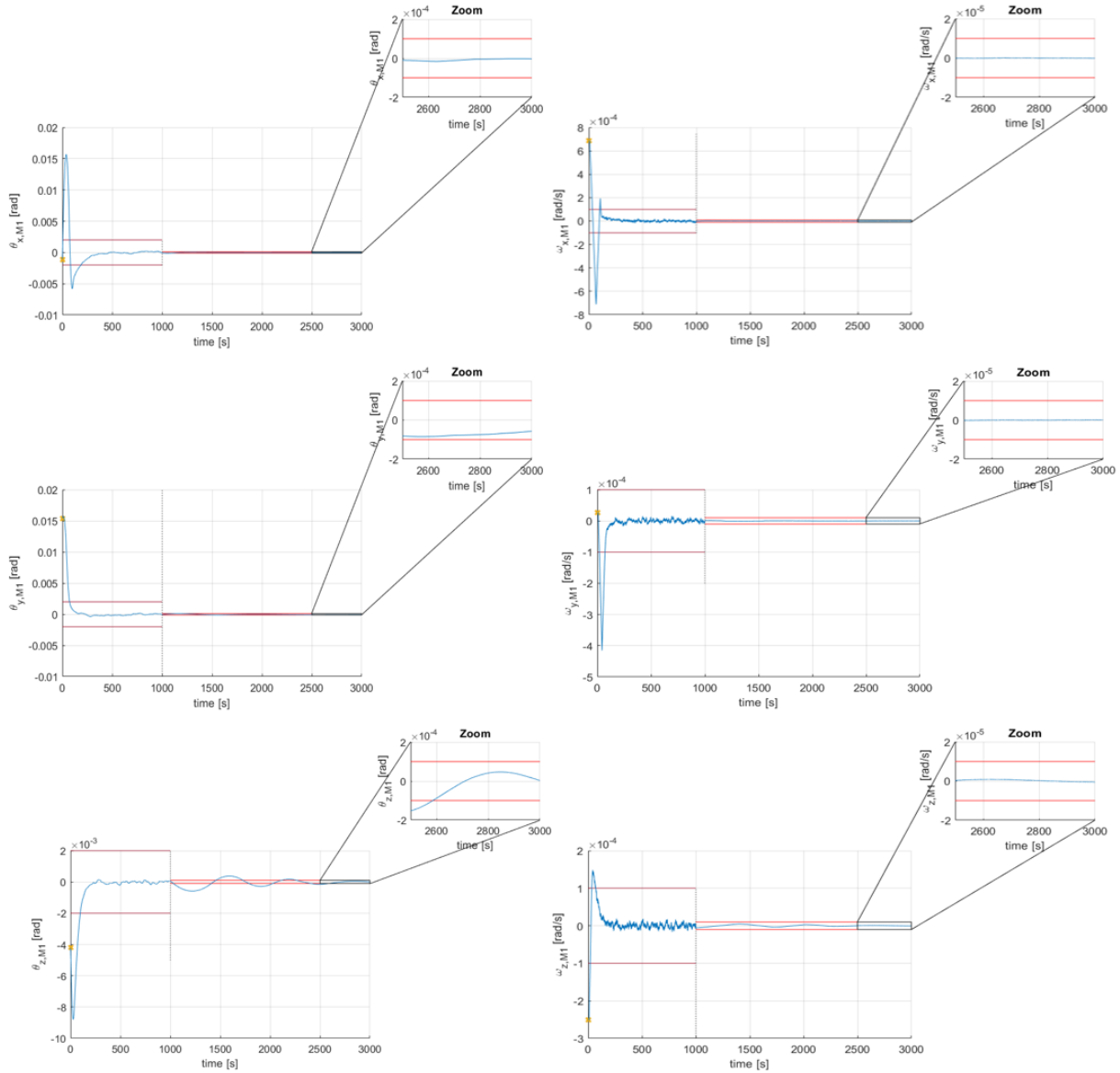


Figure 6: Variation of Euler angles and angular velocities with a 1st order SMC

presented strategy provides good results for both position and attitude control of the test mass, taking into account also external disturbances and noises due to actuators and sensors. A comparison with first order SMC is proposed to show the effectiveness of the STW-SMC in terms of accuracy and steady-state error.

## REFERENCES

- [1] F. Antonucci, M. Armano, H. Audley, G. Auger, M. Benedetti, P. Binetruy, J. Bogenstahl, D. Bortoluzzi, P. Bosetti, N. Brandt *et al.*, “The lisa pathfinder mission,” *Classical and Quantum Gravity*, vol. 29, no. 12, p. 124014, 2012.
- [2] M. Armano, H. Audley, J. Baird, P. Binetruy, M. Born, D. Bortoluzzi, E. Castelli, A. Cavalleri, A. Cesarini, A. Cruise *et al.*, “Beyond the required lisa free-fall performance: new lisa pathfinder results down to 20  $\mu$  hz,” *Physical review letters*, vol. 120, no. 6, p. 061101, 2018.
- [3] S. Vidano, C. Novara, L. Colangelo, and J. Grzysch, “The lisa dfacs: A nonlinear model for the spacecraft dynamics,” *Aerospace Science and Technology*, vol. 107, p. 106313, 2020.
- [4] A. Schleicher, T. Ziegler, R. Schubert, N. Brandt, P. Bergner, U. Johann, W. Fichter, and J. Grzysch, “In-orbit performance of the lisa pathfinder drag-free and attitude control system,” *CEAS Space Journal*, vol. 10, no. 4, pp. 471–485, 2018.
- [5] F. Montemurro, W. Fichter, M. Schlotterer, and S. Vitale, “Control design of the test mass release mode for the lisa pathfinder mission,” in *AIP Conference Proceedings*, vol. 873, no. 1. American Institute of Physics, 2006, pp. 583–587.
- [6] E. Capello, E. Punta, F. Dabbene, G. Guglieri, and R. Tempo, “Sliding-mode control strategies for rendezvous and docking maneuvers,” *Journal of Guidance, Control, and Dynamics*, vol. 40, no. 6, pp. 1481–1487, 2017.
- [7] N. Bloise, E. Capello, M. Dentis, and E. Punta, “Obstacle avoidance with potential field applied to a rendezvous maneuver,” *Applied Sciences*, vol. 7, no. 10, p. 1042, 2017.
- [8] M. Mancini, N. Bloise, E. Capello, and E. Punta, “Sliding mode control techniques and artificial potential field for dynamic collision avoidance in rendezvous maneuvers,” *IEEE Control Systems Letters*, vol. 4, no. 2, pp. 313–318, 2020.
- [9] A. Levant, “Sliding order and sliding accuracy in sliding mode control,” *International journal of control*, vol. 58, no. 6, pp. 1247–1263, 1993.
- [10] S. M. Merkowit, W. B. Haile, S. Conkey, W. Kelly III, and H. Peabody, “Self-gravity modelling for lisa,” *Classical and Quantum Gravity*, vol. 22, no. 10, p. S395, 2005.
- [11] V. I. Utkin, *Sliding modes in optimization and control problems*. Springer Verlag, New York, 1992.
- [12] Y. Shtessel, C. Edwards, L. Fridman, and A. Levant, *Sliding mode control and observation*. Springer, 2014.
- [13] G. Bartolini, E. Punta, and T. Zolezzi, “Approximability properties for second-order sliding mode control systems,” *IEEE transactions on automatic control*, vol. 52, no. 10, pp. 1813–1825, 2007.